Check for updates

Received: 8 March 2023 | Accepted: 18 September 2023

DOI: 10.1111/aos.15787

Acta Ophthalmologica

ORIGINAL ARTICLE

Retinal neurodegeneration in eyes with NPDR risk phenotypes: A two-year longitudinal study

Débora Reste-Ferreira[1] | **Inês Pereira Marques**[1,2,3,4] | **Torcato Santos**[1] | **Maria Luísa Ribeiro**[1,3,4] | **Luís Mendes**[1] | **Ana Rita Santos**[1,2,3,4,5] | **Conceição Lobo**[1,2,3,4,6] | **José Cunha-Vaz**[1,3,4]

[1]AIBILI – Association for Innovation and Biomedical Research on Light and Image, Coimbra, Portugal

[2]CORC – Coimbra Ophthalmology Reading Center, Coimbra, Portugal

[3]Coimbra Institute for Clinical and Biomedical Research (iCBR), Faculty of Medicine, University of Coimbra, Coimbra, Portugal

[4]Center for Innovative Biomedicine and Biotechnology (CIBB), University of Coimbra, Coimbra, Portugal

[5]Department of Orthoptics, School of Health, Polytechnic of Porto, Porto, Portugal

[6]Centro de Responsabilidade Integrado de Oftalmologia (CRIO), Centro Hospitalar e Universitário de Coimbra (CHUC), Coimbra, Portugal

Correspondence
José Cunha-Vaz, Association for Innovation and Biomedical Research on Light and Image, Azinhaga Sta. Comba, Celas, Coimbra 3000-548, Portugal.
Email: cunhavaz@aibili.pt

Funding information
AIBILI, COMPETE Portugal2020, Foundation for Science and Technology, Grant/Award Number: Projectno and POCI-01-0145-FEDER-030375; Fundo de Inovação, Tecnologia e Economia Circular (FITEC)—Programa Interface, Grant/Award Number: FITEC/CIT/2018/2

Abstract

Introduction: Diabetic retinopathy (DR) is both a microangiopathy and a neurodegenerative disease. However, the connections between both changes are not well known.

Purpose: To characterise the longitudinal retinal ganglion cell layer+inner plexiform layer (GCL+IPL) changes and their association with microvascular changes in type-2 diabetes (T2D) patients with nonproliferative diabetic retinopathy (NPDR).

Methods: This two-year prospective study (CORDIS, NCT03696810) included 122 T2D individuals with NPDR identified as risk phenotypes B and C, which present a more rapid progression. Phenotype C was identified by decreased VD ≥ 2SD in healthy controls, and phenotype B, identified by subclinical macular oedema with only minimal vascular closure. The GCL+IPL thickness, vessel density, perfusion density and area of intercapillary spaces (AIS) were assessed by optical coherence tomography (OCT) and OCT angiography (OCTA). Linear mixed effects models were employed to evaluate the retinal GCL+IPL progression and its associations.

Results: Regarding GCL+IPL thickness, T2D individuals presented on average 80.1 ± 7.49 μm, statistically significantly lower than the healthy control group, 82.5 ± 5.71 ($p = 0.022$), with only phenotype C differing significantly from controls ($p = 0.006$). GCL+IPL thickness steadily decreased during the two-year period in both risk phenotypes, with an annual decline rate of −0.372 μm/year ($p < 0.001$). Indeed, phenotype C showed a higher rate of progression (−0.459 μm/year, $p < 0.001$) when compared to phenotype B (−0.296 μm/year, $p = 0.036$). Eyes with ETDRS grade 20 showed GCL+IPL thickness values comparable to those of healthy control group (83.3 ± 5.80 and 82.7 ± 5.50 μm, respectively, $p = 0.880$), whereas there was a progressive decrease in GCL+IPL thickness in ETDRS grades 35 and 43–47 associated with the increase in severity of the retinopathy (−0.276 μm/year, $p = 0.004$; −0.585 μm/year, $p = 0.013$, respectively). Furthermore, the study showed statistically significant associations between the progressive thinning of GCL+IPL and the progressive increase in retinal capillary non-perfusion, with particular relevance for AIS ($p < 0.001$).

Conclusions: Our findings showed that, in eyes with NPDR and at risk for progression, retinal neurodegeneration occurs at different rates in different risk phenotypes, and it is associated with retinal microvascular non-perfusion.

KEYWORDS
diabetic retinopathy, ischaemia, neurodegeneration, NPDR, retina

This is an open access article under the terms of the Creative Commons Attribution-NonCommercial License, which permits use, distribution and reproduction in any medium, provided the original work is properly cited and is not used for commercial purposes.
© 2023 Association for Innovation and Biomedical Research on Light and Image. *Acta Ophthalmologica* published by John Wiley & Sons Ltd on behalf of Acta Ophthalmologica Scandinavica Foundation.

1 | INTRODUCTION

Diabetic retinopathy (DR) is a global epidemic pathology characterised by retinal microangiopathy and neurodegenerative changes, with a major influence on quality of life and a huge socioeconomic impact. DR is one of the leading causes of vision loss and preventable blindness worldwide in working-aged people (Cheung et al., 2010; Narayan et al., 2006). It is remarkable that DR progression occurs at different rates in different individuals, as reflected in the development of major vision-threatening complications in some patients, namely proliferative diabetic retinopathy (PDR) and diabetic macular oedema (DME) (Marques et al., 2020). The cumulative occurrence of rates of progression from mild and moderate retinopathy to vision-threatening complications has been determined to be around 14%–16%. Therefore, predicting which individuals with mild to moderate nonproliferative diabetic retinopathy (NPDR) are at risk of progression is of major relevance (Marques, Madeira, et al., 2021; Sato et al., 2001).

DR is a complex disease in which, besides microvascular alterations, neurodegeneration also appears as a relevant disease pathway (Marques et al., 2019; Marques, Kubach, et al., 2021; Simó et al., 2018; Sohn et al., 2016;). Optical coherence tomography (OCT) allows the quantification of neurodegenerative changes by measuring the thinning of the ganglion cell plus inner plexiform layers (GCL+IPL) and allows their correlation with the progression of retinal microvascular disease (Aschauer et al., 2020; Chhablani et al., 2015; Kim et al., 2019; Lim et al., 2020). In fact, it has been suggested that the DR neurodegenerative process results from diabetes-induced neuroglial activation, which leads to reduced neuronal function and apoptosis, proceeding to microvascular impairment in certain individuals (Lieth et al., 2000; Sohn et al., 2016). Our group previously reported that neurodegenerative changes occur in all DR risk phenotypes and progress steadily over time (Madeira et al., 2021; Marques et al., 2022). Different risk phenotypes of NPDR progression have been previously identified by our group as A, B and C, based on the predominance of different disease pathways. In our initial characterisation of phenotypes, the presence of microvascular changes was identified by increased microaneurysm turnover (MAT) detected by a specific algorithm, the Retmarker, not widely used (Ribeiro et al., 2022). However, to facilitate comparison of our results by other groups and to translate the information gathered into general clinical practice, we decided in this 2-year analysis to identify and characterise the ischaemia phenotype, phenotype C, by the presence of definite closure, decrease of skeletonised vessel density (SVD) in the retinal superficial capillary plexus (SVD in SCP ≥ 2 SD of healthy controls). Phenotype B was identified by the presence of subclinical macular oedema with minimal vascular closure.

In this two-year longitudinal study, we are reporting the progression of DR neurodegenerative changes in two risk phenotypes focusing on the association between neurodegenerative and microvascular changes in type 2 diabetes (T2D) individuals with mild and moderate NPDR. Only phenotype B and C, which are associated with the development of vision-threatening complications (Marques et al., 2020), were eligible in this study.

2 | METHODS

A total of 122 eyes with T2D with NPDR (levels 20, 35, 43 and 47, of the Early Treatment Diabetic Retinopathy Study (ETDRS) severity scale), one eye per patient, were eligible for the CORDIS study analysis (ClinicalTrials.gov identifier number NCT03696810). Individuals were included according to specified inclusion criteria, being identified as risk phenotype B or C, characterised based on OCT Angiography (OCTA) and OCT metrics (VD decrease ≥ 2SD and increased central retinal thickness (CRT)), and followed for two-year period with three annual visits. Individuals were excluded if significant cataract was present; a confirmed glaucoma; any eye surgery within a period of 6-months before the baseline visit, or other retinal vascular disease; any previous laser treatment or intravitreal injections, or dilation of pupil < 5 mm. Other exclusion criteria included haemoglobin A1C (HbA1c) level > 10% (85.8 mmol/mol) and any other systemic disease that could affect the eye, with special attention for uncontrolled systemic hypertension and history of heart disease. This study followed the tenets of the Declaration of Helsinki and was reviewed and approved by the AIBILI Ethics Committee for Health with the number CEC/194/18. A written informed consent was signed by each participant, after all procedures were explained. During the two-year period of the study and outside of the study visits, participants were followed in our institution in accordance with the usual clinical practice. All individuals underwent complete ophthalmological examination in annual visits, including best corrected visual acuity (BCVA), slit-lamp examination, 7-fields colour fundus photography (CFP), OCT and OCTA. Demographics data were collected, such as gender, age, duration of diabetes, co-morbidities and concomitant medication. Physical assessments were performed, including biometric measures (body weight and height) and blood pressure evaluation. Also, laboratory analyses were performed to assess metabolic control, including plasma concentrations of HbA1c and lipid fractionation identifying total cholesterol, high-density lipoprotein (HDL), low-density lipoprotein (LDL) and triglycerides.

Baseline characteristics of the study population are presented in Table 1.

2.1 | Best corrected visual acuity evaluation

The best corrected visual acuity evaluation was evaluated and recorded as letters read at 4 m on ETDRS charts. The final BCVA letter score was calculated by adding the number of letters read at 4 m plus 30 (or the number of letters read at 1 m). BCVA was assessed using the ETDRS scale and converted into logarithm units of

17553768, 2024, 4, Downloaded from https://onlinelibrary.wiley.com/doi/10.1111/aos.15787 by Estsp Politecnico Do Porto, Wiley Online Library on [09/06/2025]. See the Terms and Conditions (https://onlinelibrary.wiley.com/terms-and-conditions) on Wiley Online Library for rules of use; OA articles are governed by the applicable Creative Commons License

TABLE 1 Comparison of baseline characteristics between healthy controls and diabetic retinopathy patients divided by risk phenotypes.

	Healthy (*N*=66)	Phenotype B (*N*=65)	Phenotype C (*N*=57)	*p*–Value HvsB	*p*–Value HvsC	*p*–Value BvsC
Demographic characteristics						
Gender, male/female *N* (%)	47/19 (71.2%/28.8%)	52/13 (80.0%/20.0%)	41/16 (71.9%/28.1%)	0.310	1.000	0.394
Age (years), mean±SD	68.86±2.90	67.57±6.53	66.61±6.84	0.688	0.217	0.488
Diabetes duration (years), mean±SD	–	19.75±8.15	19.44±6.51	–	–	0.909
ETDRS levels						
ETDRS level 20	–	9 (13.8%)	3 (5.3%)			
ETDRS level 35		40 (61.5%)	34 (59.6%)	–	–	0.185
ETDRS level 43–47		16 (24.6%)	20 (35.1%)			
Systemic characteristics, mean±SD						
Body mass index (kg/m^2)		28.59±3.97	30.08±4.05			**0.010**
HbA1c (%)		7.55±1.16	7.86±1.62			0.363
Total cholesterol (mg/dL)		162.6±43.74	160.54±39.9			0.972
LDL cholesterol (mg/dL)		89.98±34.4	91.21±31.72			0.612
HDL cholesterol (mg/dL)		47.08±10.17	43.35±12.68			**0.023**
Triglycerides (mg/dL)		127.71±62.52	130.11±64.38			0.873
Systolic blood pressure (mmHg)	128.35±10.09	139.8±12.69	137.93±10.46	**<0.001**	**<0.001**	0.120
Diastolic blood pressure (mmHg)	77.35±6.76	74.12±8.73	71.33±8.21	**0.009**	**<0.001**	0.090
Ocular characteristics, mean±SD						
BCVA (logMAR)		0.00±0.08	0.03±0.09			0.218
CRT (μm)	270.52±18.07	285.6±13.1	268.8±21.8	**<0.001**	0.670	**<0.001**
GCL+IPL Thickness (μm)	82.53±5.71	81.4±6.9	78.7±7.7	0.403	**0.006**	0.069
FAZ Circularity	0.65±0.06	0.60±0.1	0.58±0.11	**0.002**	**<0.001**	0.529
FAZ Area (mm^2)	0.24±0.10	0.22±0.1	0.25±0.09	0.308	0.338	**0.026**
Vessel density – IR – SCP (mm^{-1})	22.35±0.87	21.63±0.71	19.6±0.94	**<0.001**	**<0.001**	**<0.001**
Vessel density – IR – DCP (mm^{-1})	17.26±2.16	16.78±1.60	14.82±2.22	0.165	**<0.001**	**<0.001**
Vessel density – IR – FR (mm^{-1})	23.75±0.9	23.25±0.73	21.43±0.97	**0.004**	**<0.001**	**<0.001**
Perfusion density – IR – SCP	0.40±0.02	0.40±0.02	0.38±0.02	0.894	**<0.001**	**<0.001**
Perfusion density – IR – DCP	0.33±0.04	0.32±0.03	0.29±0.04	0.370	**<0.001**	**<0.001**
Perfusion density – IR – FR	0.42±0.02	0.43±0.02	0.40±0.02	0.235	**<0.001**	**<0.001**
Area of intercapillary space – SCP (×1000 a.u.)	11.60 ± 3.18	23.02±10.06	34.35±8.61	**<0.001**	**<0.001**	**<0.001**
Area of intercapillary space – DCP (×1000 a.u.)	27.80 ± 8.53	39.25±14.11	48.43±14.36	**<0.001**	**<0.001**	**<0.001**
Area of intercapillary space – FR (×1000 a.u.)	7.52 ± 2.62	15.01±7.56	21.86±6.91	**<0.001**	**<0.001**	**<0.001**

Note: Bold values represent statistically significant alterations with $p<0.05$ using Chi-square test and Mann–Whitney U test.

Abbreviations: a.u., arbitrary unit; BCVA, best corrected visual acuity; CRT, central retinal thickness; DCP, deep capillary plexus; ETDRS, Early Treatment Diabetic Retinopathy Study; FAZ, foveal avascular zone; FR, full retina; GCL+IPL, ganglion cell layer+inner plexiform layer; HbA1c, glycated haemoglobin; HDL, high-density lipoprotein; IR, inner ring; LDL, low-density lipoprotein; *N*, number of participants; SCP, superficial capillary plexus; SD, standard deviation.

the minimal angle of resolution (logMAR). The presence of any visual loss was recorded.

2.2 | Colour fundus photography and ETDRS

ETDRS classification was based on the identification of a series of lesions (Cunha-Vaz & Mendes, 2021) and was performed based on 7-field CFP images obtained at 30/35°, using a Topcon TRC 50DX camera (Topcon Medical Systems), with a resolution of 3596×2448 pixels. The DR severity score was classified at the Coimbra Ophthalmology Reading Center (CORC) using a modified Airlie House classification scheme according to the ETDRS protocol. Classification was performed by two graders, with an inter-grader agreement of 93.7% (Santos et al., 2018).

2.3 | Optical coherence tomography and OCT-Angiography

Central retinal thickness and GCL+IPL thickness at the inner ring were measured on each participant at each visit using the Macular Cube 512×128 (512 A-scans with 128 B-scans each) acquisition protocol available on the Cirrus Zeiss 5000 AngioPlex (Carl Zeiss Meditec). Decreases (thinning) in GCL+IPL were considered to identify neurodegeneration (1SD).

OCTA vascular metrics were acquired in the central macular area using the angiography 3×3 mm acquisition protocol. This acquisition protocol consists of a set of 245 clusters of 4 B-scan repetitions, where each B-scan consists of 245 A-scans. The Carl Zeiss Meditec Density Exerciser (version:10.0.12787; Carl Zeiss

17553768, 2024, 4, Downloaded from https://onlinelibrary.wiley.com/doi/10.1111/aos.15787 by Estsp Politecnico Do Porto, Wiley Online Library on [09/06/2025]. See the Terms and Conditions (https://onlinelibrary.wiley.com/terms-and-conditions) on Wiley Online Library for rules of use; OA articles are governed by the applicable Creative Commons License

Meditec, Inc.) was used to calculate the perfusion density (PD), VD and foveal avascular zone (FAZ), detected at the superficial capillary plexus (SCP), deep capillary plexus (DCP) and full retina (FR). The area of intercapillary spaces (AIS) was calculated using the method previously described by our group (Mendes et al., 2021). Morphological operations that include the bottom-hat transform were applied to the binary slab of the en-face slabs generated by the Carl Zeiss Meditec Density Exerciser. AIS was computed for the SCP, DCP and FR.

A quality check of CRT, GCL+IPL thickness and microvascular density metrics was performed by experienced graders at our reading centre. OCT acquisitions (Macular Cube 512×128) were checked for proper alignment of the centre of the scan with the fovea location and for automated segmentation. Corrections to the results of the device automated segmentation algorithm were only performed on CRT measurements since this feature is not available in the software device for GCL+IPL thickness measurements. For OCTA acquisitions (Angiography 3×3), graders reviewed the outputs of the Carl Zeiss Meditec Density Exerciser and graded the images following the criteria: Signal Strength (SS) greater than or equal to 7, less than 25% of the imaged area grade as low-quality. Low-quality scan areas were defined as areas with unclear or defocused vessels, black spaces due to segmentation errors, cropped scans or blinking causing vessel discontinuity, duplication of vessels (ghost vessels) caused by strong eye movements and artefacts due to vitreous opacities.

Normalisation by the signal strength was accomplished in all OCTA examinations as previously described (Lei et al., 2017).

2.4 | Characterisation of diabetic retinopathy phenotypes

Diabetic retinopathy phenotypes were identified based on the values of VD in the SCP and CRT according to the following rules: phenotype C was identified by decreased values of VD of SCP ≥ 2SD of a reference healthy population and phenotype B was characterised by increased values of CRT (≥260 µm in women and ≥275 µm in men) and with minimal VD decreased in the SCP greater than 2SD of a reference healthy population (Figure 1). CRT reference values presented in this study are the reference for Zeiss Cirrus 5000 SD-OCT for subclinical macular oedema (Bandello et al., 2015; Ribeiro et al., 2015). As mentioned above, only individuals classified with phenotype B or C, which show more rapid progression, were included in the study.

2.5 | Statistical analysis

Statistical analysis was performed using Stata 16.1 (StataCorp LLC, College Station) and p-values < 0.05 were considered statistically significant. The normal distribution was assessed with the Shapiro–Wilk test and graphically verified by histogram distributions. Demographic, systemic and ocular characteristics were summarised as means and corresponding standard deviations for continuous variables and categorical variables were described as frequencies (percentage).

Accordingly, a comparison of baseline characteristics was performed for categorical variables using the chi-square test and the Mann-Whitney U test for continuous variables.

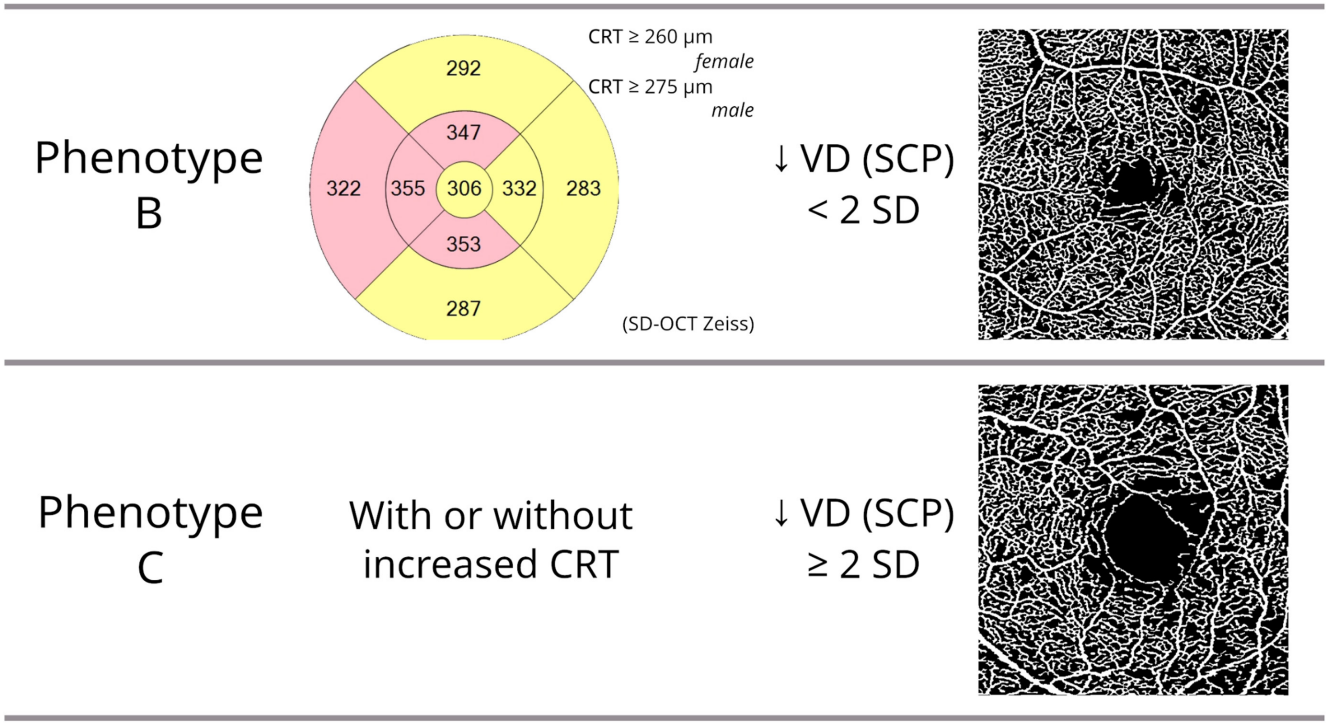

FIGURE 1 Characterisation of diabetic retinopathy risk phenotypes. Representative cases for phenotype B patients and phenotype C patients. Phenotype C was identified by decreased vessel density (VD) ≥2SD of healthy controls, and phenotype B was identified by subclinical macular oedema based on retinal thickness (CRT) with only minimal vascular closure.

17553768, 2024, 4, Downloaded from https://onlinelibrary.wiley.com/doi/10.1111/aos.15787 by Estsp Politecnico Do Porto, Wiley Online Library on [09/06/2025]. See the Terms and Conditions (https://onlinelibrary.wiley.com/terms-and-conditions) on Wiley Online Library for rules of use; OA articles are governed by the applicable Creative Commons License

A linear mixed model was applied to study longitudinal changes in GCL + IPL thickness using the restricted maximum likelihood approach (REML), where visits (baseline (0), 12-month (1) and 24-month (2)) were used as a continuous fixed variable. The results were adjusted for age, gender, diabetes durations and HbA1c, inserted as fixed covariables. The patients were used as a random effect (intercept only). Linear mixed models were applied too, using an additional fixed variable: phenotypes (B and C) or ETDRS severity groups (20, 35 and 43–47). The main effects of groups and the interactions between groups and visits were tested. Also, a linear mixed model was performed to analyse the longitudinal correlations between GCL + IPL thickness and microvascular-related variables. The effects of the predicting variables were described with beta coefficients (rates) with 95% confidence intervals (CI). To verify the linear mixed models' assumptions, homoscedasticity and normality of residuals in the models were visually inspected with residuals vs. predicted and Q-Q plots, respectively.

3 | RESULTS

Table 1 summarises the demographic, systemic and baseline ocular characteristics of the entire population enrolled in the CORDIS study. The study included a total of 122 eyes of individuals with T2D, one eye per patient, satisfying the criteria for risk phenotypes for DR progression. They were followed for a period of 2 years. There were 93 men (76.2%) and 29 women (23.8%), aged 47–79 years, and the data were compared with an age-matched healthy control population of 66 individuals, 47 men (71.2%) and 19 women (28.8%), as a reference. The patients at baseline were in the nonproliferative stage of DR (NPDR), and the eyes were classified into three groups according to the Diabetic Retinopathy Severity Scale. Twelve eyes (9.8%) were classified as ETDRS grade 20, 74 eyes (60.7%) were classified as ETDRS grade 35 and 36 (29.5%) identified as ETDRS grade 43–47. Of these, 57 eyes (47%) were further classified as phenotype C, identified by the presence of ischaemia (definite capillary closure with VD decrease ≥2SD from the normal population), and 65 eyes (53%) were classified as phenotype B, identified by the presence of subclinical macular oedema (CRT increase ≥1SD from the normal population) with absence of definite ischaemia. Of the systemic variables, HbA1c was similar in both phenotypes, and the only differences were observed in body mass index ($p = 0.010$) and high-density lipoprotein cholesterol ($p = 0.023$).

Regarding baseline GCL + IPL thickness, our results showed that the T2D individuals included in the study, representing only phenotypes B and C, presented an average of 80.1 ± 7.49 μm, statistically significantly lower

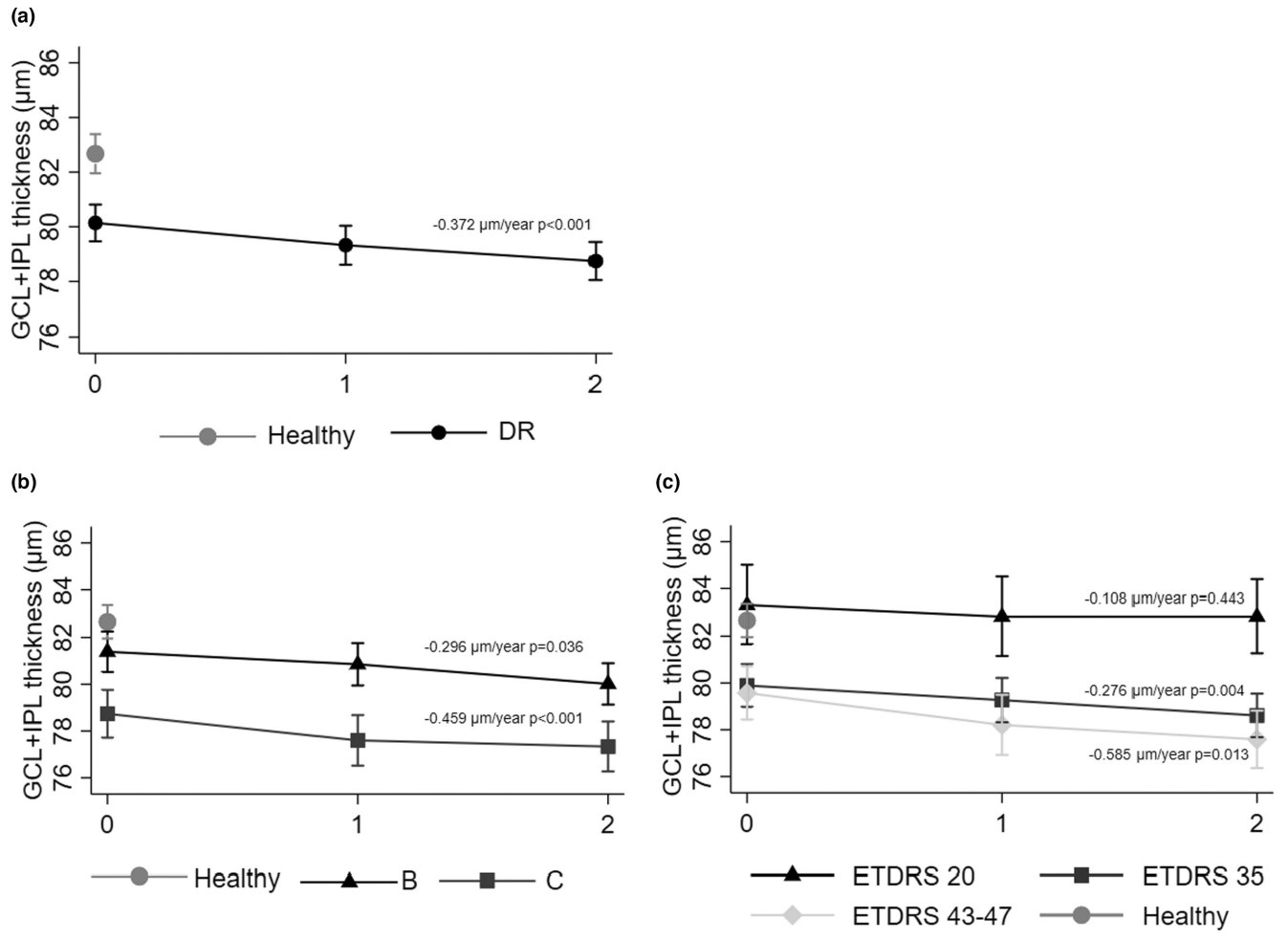

FIGURE 2 GCL + IPL thickness over a 2-year follow-up period. (a) Between healthy individuals and diabetic retinopathy patients; (b) Between the different DR phenotypes; and (c) Between the ETDRS severity groups.

17553768, 2024, 4, Downloaded from https://onlinelibrary.wiley.com/doi/10.1111/aos.15787 by Estsp Politecnico Do Porto, Wiley Online Library on [09/06/2025]. See the Terms and Conditions (https://onlinelibrary.wiley.com/terms-and-conditions) on Wiley Online Library for rules of use; OA articles are governed by the applicable Creative Commons License

TABLE 2 GCL+IPL thickness progression rates over the two-year follow-up period according to different phenotypes.

GCL+IPL thickness (μm)	*β*-Value	Change 95% confidence interval		*z*-Value	*p*-Value
Visit	−0.372	−0.530	−0.214	−4.620	**<0.001**
Phenotype B	−0.296	−0.572	−0.020	−2.10	**0.036**
Phenotype C	−0.455	−0.621	−0.289	−5.37	**<0.001**
Phenotype B vs. C	3.273	0.810	5.735	2.600	**0.009**
Phenotype B vs. C * visit	0.126	−0.103	0.355	1.080	0.281
Age (years)	−0.371	−0.563	−0.179	−3.780	**<0.001**
Gender (female vs. male)	5.141	7.934	2.349	3.610	**<0.001**
Diabetes duration (years)	0.055	−0.117	0.227	0.630	0.530
HbA1c (%)	−0.197	−0.436	0.041	−1.620	0.105

Note: Bold values represent statistically significant alterations with $p<0.05$. Linear mixed model for GCL+IPL thickness in the inner ring showing an overall progression rate of – 0.372 μm/year; visit (0–2 years) was used as a continuous fixed variable and phenotypes, age, diabetes duration, HbA1c, and gender were inserted as fixed covariates. Patients were used as a random variable (intercept only).

Abbreviations: GCL+IPL, Ganglion cell layer and Inner Plexiform Layer; HbA1c, glycated haemoglobin.

than the healthy control group, 82.5 ± 5.71 ($p=0.022$), with only phenotype C differing significantly from healthy individuals (78.7 ± 7.7 μm, $p=0.006$). As seen in Figure 2a and Table 2, the average of the GCL+IPL steadily decreased during the two-year period in both risk phenotypes. Our univariate results showed an annual decreased decline rate of −0.372 μm/year, 95% CI: [−0.530; −0.214] ($p<0.001$). When comparing the different risk phenotypes and considering thickness of GCL+IPL as an outcome (Table 2; Figure 2b), the multivariate analysis showed that age (−0.371 μm/year, 95% CI: [−0.563; −0.179], $p<0.001$) and gender were significantly associated with longitudinal changes in GCL+IPL thickness. Women showed less thinning of GCL+IPL than men (5.141 μm, 95% CI: [7.934; 2.349], $p<0.001$). It is particularly interesting to note that phenotype B differed from phenotype C (3.273 μm, 95% CI: [0.810; 5.735], $p=0.009$) and that neurodegeneration appears to decrease in parallel over 2 years in these two different risk phenotypes. Our results reported different rates of progression of the GCL+IPL thinning for the different risk phenotypes: −0.296 μm/year 95% CI: [−0.572; −0.019] for phenotype B ($p=0.036$) and −0.459 μm/year 95% CI: [−0.621; −0.289] for phenotype C ($p<0.001$).

Considering the ETDRS severity grading (Figure 2c), we identified a progressive decrease of GCL+IPL thickness in mild and moderate NPDR (ETDRS grades 35 and 43–47) which is associated with the severity of the retinopathy (−0.276 μm/year, 95% CI: [−0.464; −0.087], $p=0.004$ for ETDRS grade 35; −0.585 μm/year, 95% CI: [−1.048; −0123], $p=0.013$ for ETDRS grade 43–47), whereas eyes with minimal NPDR (ETDRS grade 20) showed GCL+IPL thickness values comparable to healthy individuals, 83.3 ± 5.80 and 82.7 ± 5.50 μm, respectively ($p=0.880$) and stable during the follow-up period (−0.108 μm/year, 95% CI: [−0.385; 0.168], $p=0.443$ for ETDRS grade 20). At baseline, no statistically significant differences were found between mild and moderate NPDR at baseline (−0.024 μm, 95% CI: [−3.082; 3.033], $p=0.987$). However, the eyes with ETDRS 43–47 showed faster GCL+IPL thinning in comparison to other ETDRS levels (ETDRS 20 $p=0.022$, and ETDRS 35 $p=0.011$).

Finally, the longitudinal associations between GCL+IPL thickness and microvascular-related variables are presented in Figure 3. There are statistically significant associations between thinning of GCL+IPL and the microvascular variables indicative of retinal capillary non-perfusion (CNP), with particular relevance for AIS. Our results showed a significant association between GCL+IPL and a decrease in VD (SCP, $p=0.009$ and DCP, $p=0.004$) and PD (SCP, DCP $p=0.006$), and an increase in AIS (SCP, DCP $p<0.001$).

4 | DISCUSSION

The present 2-year longitudinal study confirms that there is an association between neurodegenerative changes, represented by thinning of the GCL+IPL, and microvascular changes indicative of CNP. In this study, we have only included eyes identified as risk phenotypes B and C, which have been shown to be associated with increased risk of developing vision-threatening complications (Marques et al., 2020) and/or DR severity progression (Marques, Madeira, et al., 2021).

We have shown in previous studies that thinning of GCL+IPL has been present since the initial stages of NPDR and particularly in the two risk phenotypes B and C (Madeira et al., 2021). Phenotype B is identified by the presence of subclinical retinal oedema and phenotype C by a definite decrease in VD, that is, CNP. This study confirms these findings and shows that retinal neurodegeneration progresses steadily over a two-year period in these risk phenotypes, suggesting a relevant role for the neurodegenerative process since the initial stages of DR. Previous reports have, indeed, called attention to retinal neurodegeneration progression in NPDR and suggested that neuronal dysfunction could represent an early feature of DR due to primary neurodegeneration (Hellgren et al., 2014; Joltikov et al., 2017). Retinal dysfunction has been identified using standard automated perimetry (SAP) and other functional analyses. These methods provide reliable assessments of visual function early in the course of diabetic retinopathy. Joltikov et al. (2017) have also reported on the multidimensional functional and

17553768, 2024, 4, Downloaded from https://onlinelibrary.wiley.com/doi/10.1111/aos.15787 by Estsp Politecnico Do Porto, Wiley Online Library on [09/06/2025]. See the Terms and Conditions (https://onlinelibrary.wiley.com/terms-and-conditions) on Wiley Online Library for rules of use; OA articles are governed by the applicable Creative Commons License

(a)

GCL+IPL thickness	Association strength			z-value	p-value
	β-value	Change 95% confidence interval			
Vessel density - Inner Ring – SCP (mm^{-1})	0.200	0.050	0.349	2.610	**0.009**
Vessel density - Inner Ring – DCP (mm^{-1})	0.119	0.038	0.200	2.870	**0.004**
Vessel density - Inner Ring – FR (mm^{-1})	0.153	-0.006	0.311	1.880	0.060
Perfusion density - Inner Ring – SCP (a.u.)	10.238	2.960	17.517	2.760	**0.006**
Perfusion density - Inner Ring – DCP (a.u.)	6.559	1.893	11.225	2.760	**0.006**
Perfusion density - Inner Ring – FR (a.u.)	8.120	0.215	16.026	2.010	**0.044**
Area of intercapillary space – SCP (x1000 a.u.)	-3.8E-05	-5.9E-05	-1.7E-05	-3.570	**<0.001**
Area of intercapillary space – DCP (x1000 a.u.)	-2.1E-05	-3.3E-05	-0.92E-05	-3.500	**<0.001**
Area of intercapillary space – FR (x1000 a.u.)	-4.1E-05	-6.6E-05	-1.5E-05	-3.140	**0.002**

Bold values represent statistically significant alterations with $p < 0.05$. Linear mixed model of the longitudinal correlation between GCL+IPL thickness in the inner ring and microvascular-related variables; visit (0-2 years) was used as a continuous fixed variable and microvascular-related variables were inserted as fixed covariates. GCL+IPL – ganglion cell layer+ inner plexiform layer; SCP – superficial capillary plexus; DCP – deep capillary plexus; FR – full retina; a.u. – arbitrary unit.

(b)

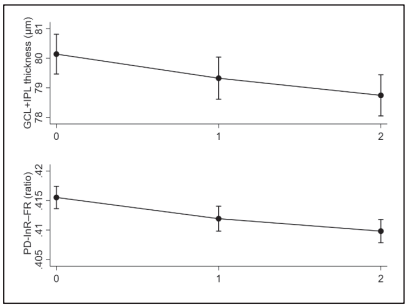

FIGURE 3 Correlations between GCL+IPL thickness and microvascular changes. (a) Longitudinal associations between changes with time (2 years) in GCL+IPL thickness and microvascular-related variables; (b) Graphical representation of the longitudinal correlation between GCL+IPL thickness and perfusion density in full retina.

structural evaluation of neuroretinal impairment in early DR. Our data suggests that an early intervention with neuroprotective agents may, indeed, be warranted to delay the retinal neurodegenerative events overring since the initial stages of the retinopathy and later as a result of CNP (Imai et al., 2009).

Previous reports have shown values for the progression of neurodegenerative changes represented by thinning of GCL+IPL in the order of −0.290 µm/year (Sohn et al., 2016) or −0.147 µm/year (Madeira et al., 2021). In the present study, the rate of progression of GCL+IPL decrease was higher than previously reported (−0.372 µm/year), which would be expected considering that only risk phenotypes characterised by rapid progression were included in the study. Indeed, phenotype C showed a higher rate of progression (−0.459 µm/year), which can be explained by the expected neurodegenerative changes resulting from the increased CNP present in these eyes. The results of this study also go a step further by identifying different rates of progression of retinal neurodegeneration within the different risk phenotypes, with a higher rate of GCL+IPL decrease verified in phenotype C, the one characterised by the presence of definite CNP. A limitation of this study is the lack of comparative longitudinal follow-up in our control group. Recent studies have reported that the thinning of GCL+IPL was significantly faster in patients with DR when compared to healthy controls (Hammel et al., 2017; Hollo & Zhou, 2016; Leung et al., 2012; Lim et al., 2020). Our reference for healthy controls is the rate of reduction of the average GCL+IPL thickness reported by Lim et al. (−0.277 µm/year) (Lim et al., 2020) and by Hammel et al. (−0.14 µm/year) (Hammel et al., 2017).

Understanding the link between neuronal and vascular damage is crucial for the clinical definition of DR and to identify novel therapeutic agents for early intervention, slowing or preventing the development of DR. The retinal neurodegeneration identified in diabetic retinopathy can be interpreted as a synchronised process. Apparently, in the most initial stages, there is progressive GCL+IPL thinning, which is associated with the progression of the retinopathy and may play a role in triggering the development of the microvascular changes. Diabetic retinopathy has been generally considered to be a microvascular disease, initiated by changes in the blood vessels and the breakdown of the blood-retinal barrier (Cunha-Vaz et al., 1979). Our study shows that neurodegenerative changes in the retina, manifested by progressively increased GCL+IPL thinning, occur with disease progression particularly in eyes with definite CNP. Combined information on the degree of neurodegenerative changes and information on the degree of CNP may, indeed, offer an opportunity for improved characterisation of DR progression, replacing the ETDRS classification with information that can be obtained in an independent and automated form using OCT and OCTA data, as previously proposed by our group (Cunha-Vaz & Mendes, 2021).

The population studied was relatively well controlled, using exclusion criteria such as excessive HbA1c levels (10%) and uncontrolled blood pressure. This may be also considered an advantage as it decreases the influence of extreme systemics factors.

5 | CONCLUSIONS

The observations here reported offer relevant new perspectives for personalised management of NPDR, suggesting opportunities to prevent its progression before the development of vision-threatening complications. The presence and degree of CNP demonstrated by OCTA and the identification of rapidly progressing neurodegeneration identified by changes in GCL+IPL using OCT parameters can be obtained non-invasively and are able to identify risk phenotypes that are associated with more rapid disease progression. Furthermore, the identification of high-risk phenotypes of NPDR offers a promising opportunity for closer follow-up to monitor progression and open the door for the development of novel therapeutic strategies.

AUTHOR CONTRIBUTIONS

Débora Reste-Ferreira, Inês Pereira Marques, Torcato Santos, Maria Luísa Ribeiro, Luís Mendes and Ana Rita

17553768, 2024, 4, Downloaded from https://onlinelibrary.wiley.com/doi/10.1111/aos.15787 by Estsp Politecnico Do Porto, Wiley Online Library on [09/06/2025]. See the Terms and Conditions (https://onlinelibrary.wiley.com/terms-and-conditions) on Wiley Online Library for rules of use; OA articles are governed by the applicable Creative Commons License

Santos collected data, analysed, wrote and reviewed and edited the manuscript. Conceição Lobo and José Cunha-Vaz assisted in the analysis and interpretation of the data and wrote the manuscript. José Cunha-Vaz is the guarantor of this work and, as such, had full access to all the data in the study and takes responsibility for the integrity of the data and the accuracy of the data analysis. All authors have read and agreed to the published version of the manuscript.

FUNDING INFORMATION

This work was supported by AIBILI, COMPETE Portugal2020, Foundation for Science and Technology (Project no: POCI-01-0145-FEDER-030375) and the Fundo de Inovação, Tecnologia e Economia Circular (FITEC)—Programa Interface (FITEC/CIT/2018/2). No funding or sponsorship was received for the publication of this article.

CONFLICT OF INTEREST STATEMENT

Débora Reste-Ferreira, Inês Pereira Marques, Torcato Santos, Maria Luísa Ribeiro, Luís Mendes, Ana Rita Santos and Conceição Lobo declare no conflicts of interest. José Cunha-Vaz reports grants from Carl Zeiss Meditec and is a consultant for Alimera Sciences, Bayer, Novartis, Roche and Carl Zeiss Meditec. The funders had no role in the design or writing of the manuscript.

DATA AVAILABILITY STATEMENT

The datasets generated during and/or analysed during the current study are available from the corresponding author on reasonable request.

AUTHORSHIP

All named authors meet the International Committee of Medical Journal Editors (ICMJE) criteria for authorship for this article, take responsibility for the integrity of the work as a whole and have given their approval for this version to be published.

INFORMED CONSENT STATEMENT

Written informed consent was obtained by each participant agreeing to participate in the study.

INSTITUTIONAL REVIEW BOARD STATEMENT

The tenets of the Declaration of Helsinki were followed, and approval was obtained from the AIBILI Ethics Committee for Health with the number NCT03696810 (ClinicalTrials.gov identifier).

ORCID

José Cunha-Vaz https://orcid.org/0000-0002-0947-9850

REFERENCES

Aschauer, J., Pollreisz, A., Karst, S., Hülsmann, M., Hajdu, D., Datlinger, F. et al. (2020) Longitudinal analysis of microvascular perfusion and neurodegenerative changes in early type 2 diabetic retinal disease. *British Journal of Ophthalmology*, 106(4), 528–533. Available from: https://doi.org/10.1136/bjophthalmol-2020-317322

Bandello, F., Tejerina, A.N., Vujosevic, S., Varano, M., Egan, C., Sivaprasad, S. et al. (2015) Retinal layer location of increased retinal thickness in eyes with subclinical and clinical macular edema in diabetes type 2. *Ophthalmic Research*, 54(3), 112–117. Available from: https://doi.org/10.1159/000438792

Cheung, N., Mitchell, P. & Wong, T.Y. (2010) Diabetic retinopathy. *The Lancet*, 376, 124–136. Available from: https://doi.org/10.1016/S0140-6736(09)62124-3

Chhablani, J., Sharma, A., Goud, A., Peguda, H.K., Rao, H.L., Begum, V.U. et al. (2015) Neurodegeneration in type 2 diabetes: evidence from spectral-domain optical coherence tomography. *Investigative Ophthalmology and Visual Science*, 56(11), 6333–6338. Available from: https://doi.org/10.1167/iovs.15-17334

Cunha-Vaz, J. & Mendes, L. (2021) Characterization of risk profiles for diabetic retinopathy progression. *Journal of Personalized Medicine*, 11(8), 826. Available from: https://doi.org/10.3390/jpm11080826

Cunha-Vaz, J.G., Goldberg, M.F., Vygantas, C. & Noth, J. (1979) Early detection of retinal involvement in diabetes by vitreous fluorophotometry. *Ophthalmology*, 86(2), 264–275.

Hammel, N., Belghith, A., Weinreb, R.N., Medeiros, F.A., Mendoza, N. & Zangwill, L.M. (2017) Comparing the rates of retinal nerve fiber layer and ganglion cell-inner plexiform layer loss in healthy eyes and in glaucoma eyes. *American Journal of Ophthalmology*, 178, 38–50. Available from: https://doi.org/10.1016/j.ajo.2017.03.008

Hellgren, K.J., Agardh, E. & Bengtsson, B. (2014) Progression of early retinal dysfunction in diabetes over time: results of a long-term prospective clinical study. *Diabetes*, 63(9), 3104–3111. Available from: https://doi.org/10.2337/db13-1628

Hollo, G. & Zhou, Q. (2016) Evaluation of retinal nerve fiber layer thickness and ganglion cell complex progression rates in healthy, ocular hypertensive, and glaucoma eyes with the Avanti RTVue-XR optical coherence tomograph based on 5-year follow-up. *Journal of Glaucoma*, 25(10), e905–e909. Available from: https://doi.org/10.1097/IJG.0000000000000410

Imai, H., Singh, R.S.J., Fort, P.E. & Gardner, T.W. (2009) Neuroprotection for diabetic retinopathy. *Developments in Ophthalmology*, 44, 56–68. Available from: https://doi.org/10.1159/000223946

Joltikov, K.A., de Castro, V.M., Davila, J.R., Anand, R., Khan, S.M., Farbman, N. et al. (2017) Multidimensional functional and structural evaluation reveals neuroretinal impairment in early diabetic retinopathy. *Investigative Ophthalmology and Visual Science*, 58(6), BIO277–BIO290. Available from: https://doi.org/10.1167/iovs.17-21863

Kim, K., Kim, E.S., Kim, D.G. & Yu, S.Y. (2019) Progressive retinal neurodegeneration and microvascular change in diabetic retinopathy: longitudinal study using OCT angiography. *Acta Diabetologica*, 56(12), 1275–1282. Available from: https://doi.org/10.1007/s00592-019-01395-6

Lei, J., Durbin, M.K., Shi, Y., Uji, A., Balasubramanian, S., Baghdasaryan, E. et al. (2017) Repeatability and reproducibility of superficial macular retinal vessel density measurements using optical coherence tomography angiography en face images. *JAMA Ophthalmology*, 135(10), 1092–1098. Available from: https://doi.org/10.1001/jamaophthalmol.2017.3431

Leung, C.K.S., Yu, M., Weinreb, R.N., Ye, C., Liu, S., Lai, G. et al. (2012) Retinal nerve fiber layer imaging with spectral-domain optical coherence tomography: a prospective analysis of age-related loss. *Ophthalmology*, 119(4), 731–737. Available from: https://doi.org/10.1016/j.ophtha.2011.10.010

Lieth, E., Gardner, T.W., Barber, A.J. & Antonetti, D.A. (2000) Retinal neurodegeneration: early pathology in diabetes. *Clinical and Experimental Ophthalmology*, 28(1), 3–8. Available from: https://doi.org/10.1046/j.1442-9071.2000.00222.x

Lim, H.B., Shin, Y.I., Lee, M.W., Koo, H., Lee, W.H. & Kim, J.Y. (2020) Ganglion cell – inner plexiform layer damage in diabetic patients: 3-year prospective, longitudinal, observational study. *Scientific Reports*, 10(1), 1–9. Available from: https://doi.org/10.1038/s41598-020-58465-x

Madeira, M.H., Marques, I.P., Ferreira, S., Tavares, D., Santos, T., Santos, A.R. et al. (2021) Retinal neurodegeneration in different risk phenotypes of diabetic retinal disease. *Frontiers in Neuroscience*, 15, 800004. Available from: https://doi.org/10.3389/fnins.2021.800004

17553768, 2024, 4, Downloaded from https://onlinelibrary.wiley.com/doi/10.1111/aos.15787 by Estsp Politecnico Do Porto, Wiley Online Library on [09/06/2025]. See the Terms and Conditions (https://onlinelibrary.wiley.com/terms-and-conditions) on Wiley Online Library for rules of use; OA articles are governed by the applicable Creative Commons License

Marques, I.P., Alves, D., Santos, T., Mendes, L., Santos, A.R., Lobo, C. et al. (2019) Multimodal imaging of the initial stages of diabetic retinopathy: different disease pathways in different patients. *Diabetes*, 68(3), 648–653. Available from: https://doi.org/10.2337/db18-1077

Marques, I.P., Ferreira, S., Santos, T., Madeira, M.H., Santos, A.R., Mendes, L. et al. (2022) Association between neurodegeneration and macular perfusion in the progression of diabetic retinopathy: a 3-year longitudinal Study. *Ophthalmologica*, 245(4), 335–341. Available from: https://doi.org/10.1159/000522527

Marques, I.P., Kubach, S., Santos, T., Mendes, L., Madeira, M.H., de Sisternes, L. et al. (2021) Optical coherence tomography angiography metrics monitor severity progression of diabetic retinopathy—3-year longitudinal study. *Journal of Clinical Medicine*, 10(11), 2296. Available from: https://doi.org/10.3390/jcm10112296

Marques, I.P., Madeira, M.H., Messias, A.L., Martinho, A.C.V., Santos, T., Sousa, D.C. et al. (2021) Different retinopathy phenotypes in type 2 diabetes predict retinopathy progression. *Acta Diabetologica*, 58(2), 197–205. Available from: https://doi.org/10.1007/s00592-020-01602-9

Marques, I.P., Madeira, M.H., Messias, A.L., Santos, T., Martinho, A.C.V., Figueira, J. et al. (2020) Retinopathy phenotypes in type 2 diabetes with different risks for macular edema and proliferative retinopathy. *Journal of Clinical Medicine*, 9(5), 1433. Available from: https://doi.org/10.3390/jcm9051433

Mendes, L., Marques, I.P. & Cunha-Vaz, J. (2021) Comparison of different metrics for the identification of vascular changes in diabetic retinopathy using OCTA. *Frontiers in Neuroscience*, 15, 755730. Available from: https://doi.org/10.3389/fnins.2021.755730

Narayan, K.M.V., Boyle, J.P., Geiss, L.S., Saaddine, J.B. & Thompson, T.J. (2006) Impact of recent increase in incidence on future diabetes burden: U.S., 2005-2050. *Diabetes Care*, 29(9), 2114–2116. Available from: https://doi.org/10.2337/dc06-1136

Ribeiro, L., Bandello, F., Tejerina, A.N., Vujosevic, S., Varano, M., Egan, C. et al. (2015) Characterization of retinal disease progression in a 1-year longitudinal study of eyes with mild nonproliferative retinopathy in diabetes type 2. *Investigative Ophthalmology and Visual Science*, 56(9), 5698–5705. Available from: https://doi.org/10.1167/iovs.15-16708

Ribeiro, L., Marques, I.P., Santos, T., Carvalho, S., Santos, A.R., Mendes, L. et al. (2022) Characterization of two-year progression of different phenotypes of nonproliferative diabetic retinopathy. *Ophthalmic Research*, 66(1), 228–237. Available from: https://doi.org/10.1159/000526370

Santos, A.R., Costa, M.Â., Schwartz, C., Alves, D., Figueira, J., Silva, R. et al. (2018) Optical coherence tomography baseline predictors for initial best-corrected visual acuity response to intravitreal anti-vascular endothelial growth factor treatment in eyes with diabetic macular edema: the CHARTRES Study. *Retina*, 38(6), 1110–1119. Available from: https://doi.org/10.1097/IAE.0000000000001687

Sato, Y., Lee, Z. & Hayashi, Y. (2001) Subclassification of preproliferative diabetic retinopathy and glycemic control: relationship between mean hemoglobin A1C value and development of proliferative diabetic retinopathy. *Japanese Journal of Ophthalmology*, 45(5), 523–527. Available from: https://doi.org/10.1016/s0021-5155(01)00380-x

Simó, R., Stitt, A.W. & Gardner, T.W. (2018) Neurodegeneration in diabetic retinopathy: does it really matter? *Diabetologia*, 61(9), 1902–1912. Available from: https://doi.org/10.1007/s00125-018-4692-1

Sohn, E.H., van Dijk, H.W., Jiao, C., Kok, P.H.B., Jeong, W., Demirkaya, N. et al. (2016) Retinal neurodegeneration may precede microvascular changes characteristic of diabetic retinopathy in diabetes mellitus. *Proceedings of the National Academy of Sciences*, 113(19), E2655–E2664. Available from: https://doi.org/10.1073/pnas.1522014113

How to cite this article: Reste-Ferreira, D., Marques, I.P., Santos, T., Ribeiro, M.L., Mendes, L., Santos, A.R. et al. (2024) Retinal neurodegeneration in eyes with NPDR risk phenotypes: A two-year longitudinal study. *Acta Ophthalmologica*, 102, e539–e547. Available from: https://doi.org/10.1111/aos.15787

17553768, 2024, 4, Downloaded from https://onlinelibrary.wiley.com/doi/10.1111/aos.15787 by Estsp Politecnico Do Porto, Wiley Online Library on [09/06/2025]. See the Terms and Conditions (https://onlinelibrary.wiley.com/terms-and-conditions) on Wiley Online Library for rules of use; OA articles are governed by the applicable Creative Commons License